This is a non-peer reviewed preprint submitted to EarthXiv

CRUSTAL ACCRETION AND CHAIN BUILDING OF AN INHERITED PASSIVE MARGIN: INSIGHTS FROM THE WESTERN SOUTHERN ALPS

Emanuele Scaramuzzo[1*], Franz A. Livio[1], Pablo Granado[2], Raffaele Bitonte[1,3] and Andrea Di Capua[1, 4]

1 - Università degli Studi dell'Insubria, Dipartimento di Scienza ed Alta Tecnologia, via Valleggio 11, 22100, Como, Italy

2 - Institut de Recerca Geomodels, Departament de Dinàmica de la Terra i de l'Oceà, Universitat de Barcelona, Marti i Franques s/n, 08028 Barcelona, Spain

3 - Edison Exploration & Production Spa Foro Buonaparte 31, 20121 Milan – Italy

4 - CNR - Institute of Environmental Geology and Geoengineering, Via Mario Bianco 9, 20131, Milan, Italy

Corresponding Author: Emanuele Scaramuzzo escaramuzzo@uninsubria.it

ABSTRACT

Recently, the influence of lithospheric extension on later orogeny has gained increasing interest. We make use of own geological mapping, interpretations of seismic reflection profiles and deep geophysical data to build an area-balanced cross-section across a key area of the Western Southern Alps and to model a series of structural restorations from the end of Mesozoic rifting to present-day. The interpreted ramp-dominated and basement-involved style results during retro-wedge accretion through reactivation of long-lived inherited structures. Early phases of Alpine orogeny resulted in north-verging reactivation of Early Permian structures and Triassic-Jurassic extensional basins, whereas later phases led to the internal deformation of the orogenic retro-wedge. Our results also suggest that, during the collisional and post-collisional tectonics, lithosphere dynamics drove diachronically the onset of tectonic phases (i.e., wedging and slab retreat), from east to west, across the Western Southern Alps.

INTRODUCTION

An increasing interest has been recently focused in literature on the role of lithospheric extension and inheritance in affecting later orogeny (e.g., Roda et al., 2019; Festa et al., 2020; Lescoutre and Manatschal, 2020; Tavani et al., 2021); nonetheless, most of the structural interpretations of the orogenic chains worldwide are still based on the old concepts arising from the hydrocarbons prospection studies and traditionally divided into thick vs thin skinned models. In more recent years, considering the whole scale orogen, continental lithospheric contractional styles have been rather conceptualized as ranging between two end-members scenarios that describe the distribution of strain with depth, down to the lithosphere boundary, and resulting in different amounts and geometries of crustal accretion in orogenic wedges: detachment-dominated, and ramp-dominated scenarios (Butler and Mazzoli, 2006). Such a conceptual model can better describe the evolution of a whole orogenic system, including the role of inherited lithospheric anisotropies, if a crustal-scale section can be effectively built. The aim of this work relies on the application of these recent views in a key area of the European Western Southern Alps, supported by geological mapping, geophysics and seismology.

The Western Southern Alps are a natural laboratory for observing the involvement of an ancient passive margin in an orogenic wedge. The Ivrea Zone (Fig. 1a) represents an upright section of exhumed upper mantle lenses and lower continental crustal rocks, and is correlated at depth with a denser body of mantle rocks (i.e. the so-called Ivrea Body) that could represent the north-western tip of Adria's upper mantle (e.g. Handy et al., 1999; Schaltegger and Brack, 2007; Schmid et al., 2017). To the east, where extensive Permian-Mesozoic cover units crop out, the Southern Alps have been classically interpreted as a tapered tectonic wedge composed of a stacked pile of nappes involving thin slices of basement and cover units (Schumacher et al., 1997; Rosenberg and Kissling, 2013; Pfiffner, 2016), even though not directly constrained by any deep wells or seismic data.

In this contribution, we report on the *Varese area* (Fig. 1b) where we have mapped in detail the Mesozoic cover and its autochthonous upper crustal basement and have integrated available geophysical data to provide a new crustal-scale cross section. We then performed a progressive structural restoration to decipher timing and partitioning of deformation among different crustal levels, which allows defining an alternative model for the evolution of the Western Southern Alps.

GEOLOGICAL SETTING

The Western Southern Alps (Fig.1a) are located at the north-western border of the Adria plate and are bound to the northwest by the Canavese Line (e.g. Schmid et al., 1987). The basement of the Western Southern Alps includes a series of tectono-metamorphic units which assembled during the Variscan orogeny (e.g. Schaltegger and Brack, 2007). Lower crustal units of the Ivrea Zone represent a heterogeneous suite of high-grade metamorphic rocks whereas upper crustal portions are represented by Variscan related units. The Adriatic basement was intruded by basic-to-acid igneous bodies (Karakas et al., 2019) during the Early Permian (280-285 Ma) and was covered by volcanogenic deposits (Schaltegger and Brack, 2007). The Cossato-Mergozzo-Brissago (Fig. 1a; Schaltegger and Brack, 2007; Mazzucchelli et al., 2014) is a major crustal shear zone formed during this time in the Ivrea Zone, related to crustal thinning and a first pulse of lower crust exhumation (Handy et al., 1999) and other Early Permian extensional faults are reported as well more to the east (Pohl et al., 2018).

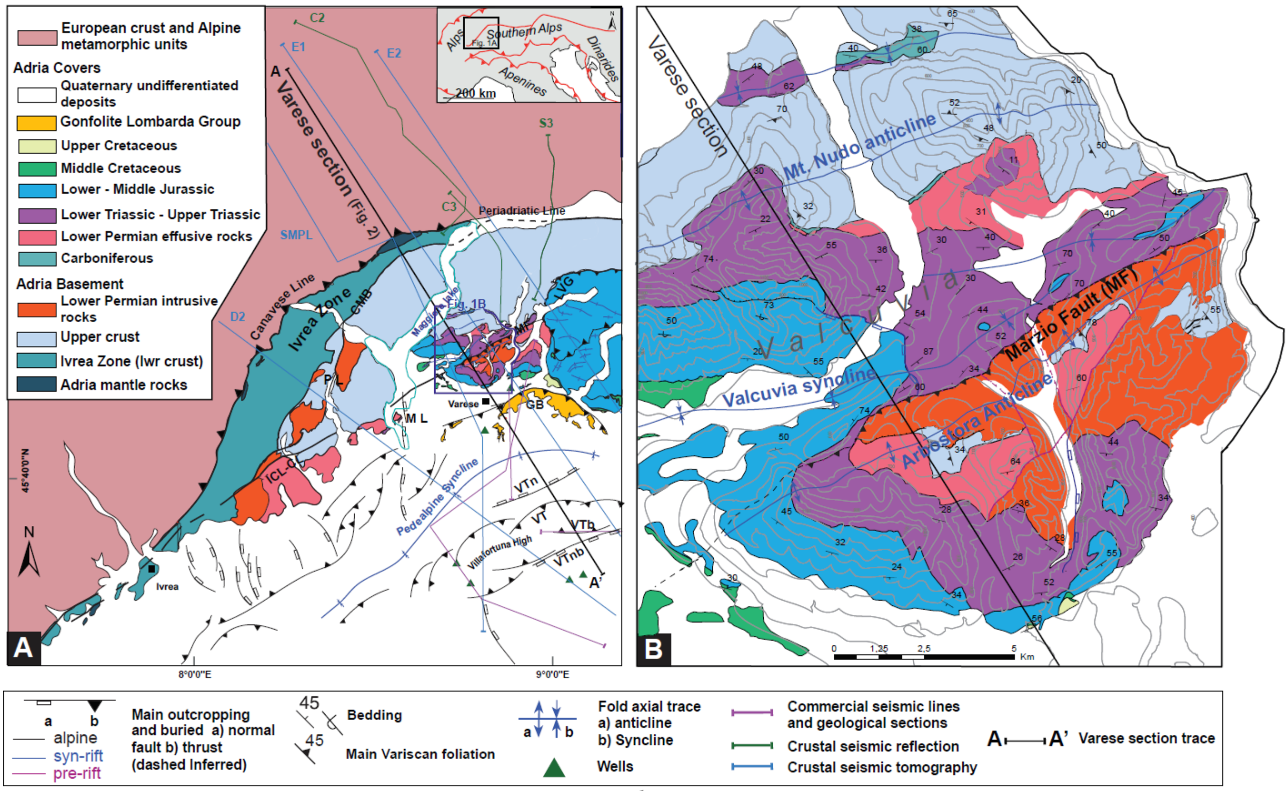

Figure 1: Figure 1: a) Geology of the Western Southern Alps with traces of the seismic reflection lines and wells used for construction of the Varese cross-section; b) simplified geological map of the Varese area. Codes: CMB, Cossato Mergozzo Line; GB, Gonfolite backthrust; ICL-CL, Internal Canavese Line-Cremosina Line; LVG, Lugano Valgrande fault; MF, Marzio Fault; ML, Maggiore Line; PL, Pogallo Line; VCL, Val Colla Line; VT and VTb, Villafortuna Trecate Thrust and Backthrust (based on Fantoni et al., 2002; Mazzucchelli et al., 2014).

During the Late Permian-Early Triassic, a regional transgression affected the area with the deposition of siliciclastic and carbonate deposits (Bertotti et al., 1993). Late Triassic to Jurassic rifting led to the formation of the Alpine Tethys passive margin and dismembered the Adriatic crust into a series of basins and swells separated by N-S striking listric normal faults (e.g., Fantoni and Scotti, 2009), namely the Pogallo Line, Maggiore Line and the Lugano-Valgrande fault (Fig. 1a). Some of these faults were already formed in Permian times and became subsequently reactivated during this rifting event (e.g. Schaltegger and Brack, 2007) whereas new faults were also formed. These fault systems were associated with a second pulse of crustal attenuation and extensional exhumation of the lower and intermediate crust and resulted in the deposition of thick Lower Jurassic syn-rift sequences (Berra et al., 2009). The Varese section shows a change in the associated depocenters, from a Permian-Triassic basin in south of the Marzio Fault (Fig. 1b), to a Jurassic half graben immediately north of this fault. In response to the Cretaceous subduction and the Oligocene

Europe-Adria indentation, the lower and upper crustal sections of the Adriatic plate were tilted, overturned and exhumed along presently steeply dipping shear zones (Schmid et al. 1996, 2017).

RESULTS

The Varese Section

We built the Varese section by integrating surface geology (Fig. 1b) and shallow seismic reflection profiles tied to available well logs and deeper-reaching geophysical data including a 3-D high-resolution P-wave tomography of the Alpine crust (Diehl et al., 2009; 2017, Rosenberg and Kissling, 2013). Moho depth is that mapped by Spada et al. (2013) and well-constrained earthquake *foci* for the 1985 to 2020 period, within a 30 km wide corridor (ISIDe Database). Following Diehl et al. (2009), we define the boundary between lower and upper Adria crust by the 6.5 km/s Vp contour line, where other external constraints are lacking. The Triassic cover units, unconformably overlying the metamorphic basement and Permian intrusive bodies, have a thickness of ca. 2-3 km and are overlain by a syn- to post-rift sequence up to 3 km of thickness (Fig. 1b). Basement and cover units are involved in a north-verging reverse fault-propagation-fold related to the Marzio Fault (Fig. 2). The Marzio Fault represents the easternmost segment of a fault system aligned with the Internal Canavese and Cremosina lines (Fig. 1a) that were active since upper Carboniferous (?) - Permian (e.g., Festa et al., 2020). The Marzio Fault bounds a sub-volcanic Early Permian body (Schaltegger and Brack 2007) suggesting structural control during its emplacement. To the west, the Marzio Fault is concealed in a 2 km-thick zone of distributed deformation within the syn-rift units (Fig. 1b).

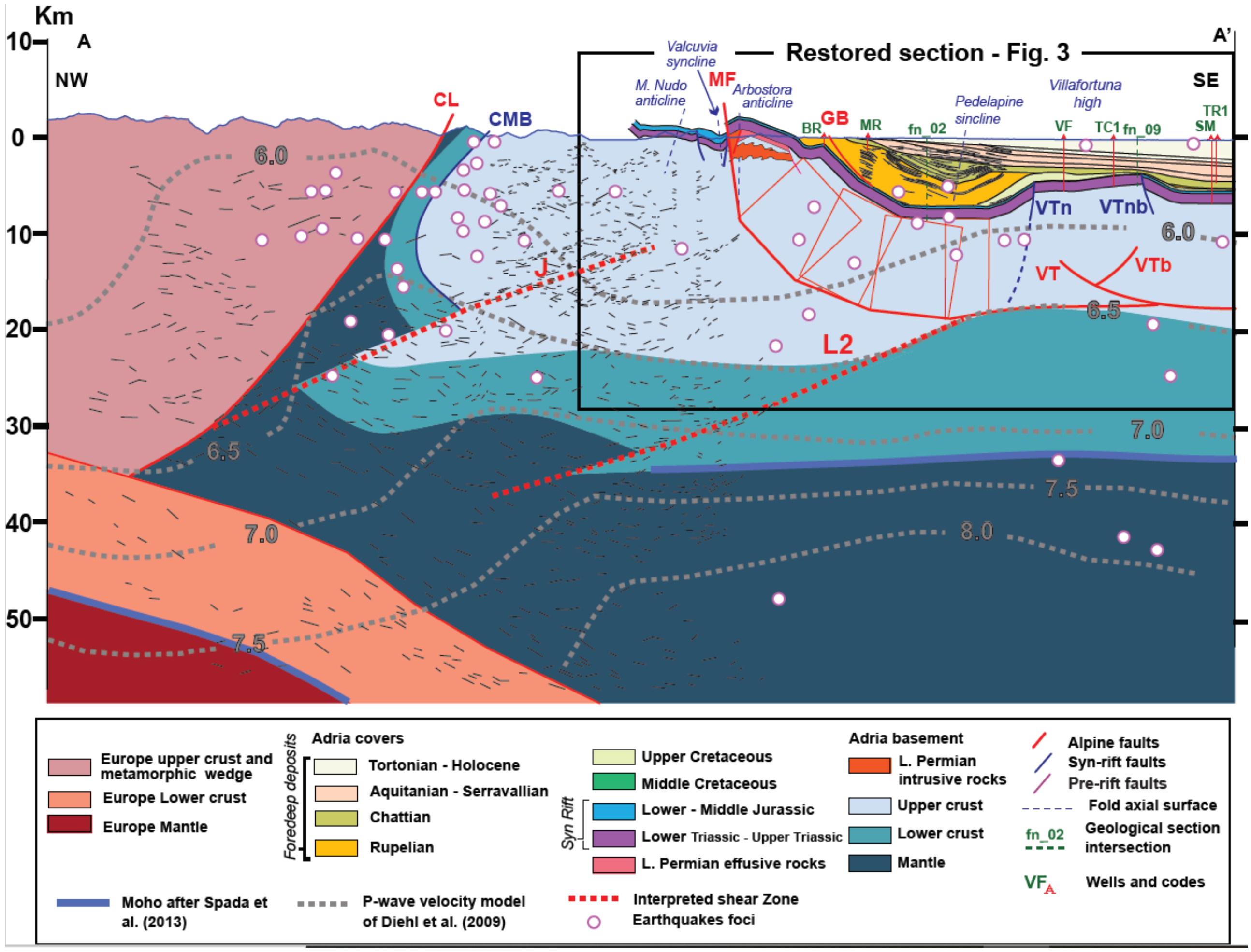

Figure 2: Varese section (trace in Fig. 1a); line drawing from reflection profiles C2, C3 and S3 of the NFP20 project (Pfiffner et al., 1997) and from a reflection profile in the Gonfolite Gr. are reported; J and L2 indicate crustal shear zones and the red boxes represent the dip panel used for deriving the deep geometry of the Marzio fault (see text for details). Codes are the same as in Figure 1.

On the hanging wall of the Marzio Fault to the south, the NE-SW trending asymmetric Arbostora anticline runs for more than 20 km along strike, plunging 22° towards N235E and displaying a wavelength of *ca.* 25 km. The Arbostora anticline involves the entire Permian and Mesozoic sequence (Fig. 1b), suggesting a deep-seated detachment. On the other hand, the Pedealpine syncline in the Po Plain to the south (Fig. 1) hosts the South Alpine sediments of the Oligocene-Miocene Gonfolite Lombarda Group (Tremolada et al., 2010); these sediments are deformed by thrusts rooted at shallower levels such as the Gonfolite backthrust (Fig. 2, e.g., Fantoni et al., 2002).

We constrained the geometry of the Marzio Fault at depth by adopting a construction method whereby hanging wall rocks follow displacement trajectories parallel to the fault line at depth (Fig. 2). We obtained a thick-skinned N-verging high-angle reverse fault, with an associated hanging wall harpoon anticline related to the positive inversion of the Marzio Fault, resembling a break-through fault-propagation fold with a maximum structural relief of *ca.* 10 km in respect to the base of the Pedealpine syncline (Fig. 2).

North of this regional structure we traced two well-defined deep-seated northwest-dipping seismic reflectors (J and L2 in Fig. 2) that have been previously recognized and interpreted as shear zones in the deep seismic reflection profile NFP20 (sections S3 and C3 in Pfiffner et al., 1997; Schumacher, et al., 1997). We interpreted the positive reactivation of the Marzio Fault to be kinematically linked with the L2 shear zone, constituting as a crustal-scale wedge (Fig. 2). The L2 shear zone would dip northwestwards and cross the Moho boundary, separating domains with differing lower crustal thicknesses. Stacking of thin lower crustal slices attached to their corresponding upper crust can also provide a similar upwarping of Vp trajectories below the Ivrea Zone.

Beside the steeply dipping Marzio Fault indicative of back-tiling, basement-involved folding to the north is represented by the Valcuvia syncline and the Mt. Nudo anticline (Fig. 2). In this sector, changes in the Permian-Triassic and Jurassic thickness distribution suggest the presence of a Jurassic rift fault (Fig. 3) that also would have undergone positive tectonic inversion during crustal wedging. Seismic reflector J should correspond to a major shear zone in the core of the upright to overturned Adria crust. Slip along this shear zone would ideally provide both uplift and folding of the northern sector and back-tilting of the Marzio Fault and its hanging wall. Crustal stacking and wedging, including the positive reactivation of the Marzio Fault as a back-thrust in the wedge's tip, would have formed the Pedealpine syncline, where Oligocene-Miocene syn-orogenic deposits accumulated. A major pulse of uplift related to such crustal wedging is recorded in the Pedealpine syncline by the large erosional unconformity at the base of the Aquitanian, as well as the development of the Gonfolite backthrust resulting from flexural slipping and out-of-the syncline thrusting.

KINEMATIC RESTORATION: INSIGHTS ON THE TECTONIC EVOLUTION OF THE WESTERN SOUTHERN ALPS

We have tested our model through a progressive kinematic restoration of a simplified version of the Varese section (Fig. 3 and Appendix file for the restoration methods). We restored the section in 5 steps from present-day to the end of the Jurassic rifting, by means of a kinematic approach and using dated horizons in the Gonfolite Lombarda Group as reference horizons. We restored faults and shear zones as trishear structures (Zehnder and Allmendinger, 2000), a kinematic model previously applied to other contractional basement-involved structures worldwide (e.g., Mitra and Miller 2013).

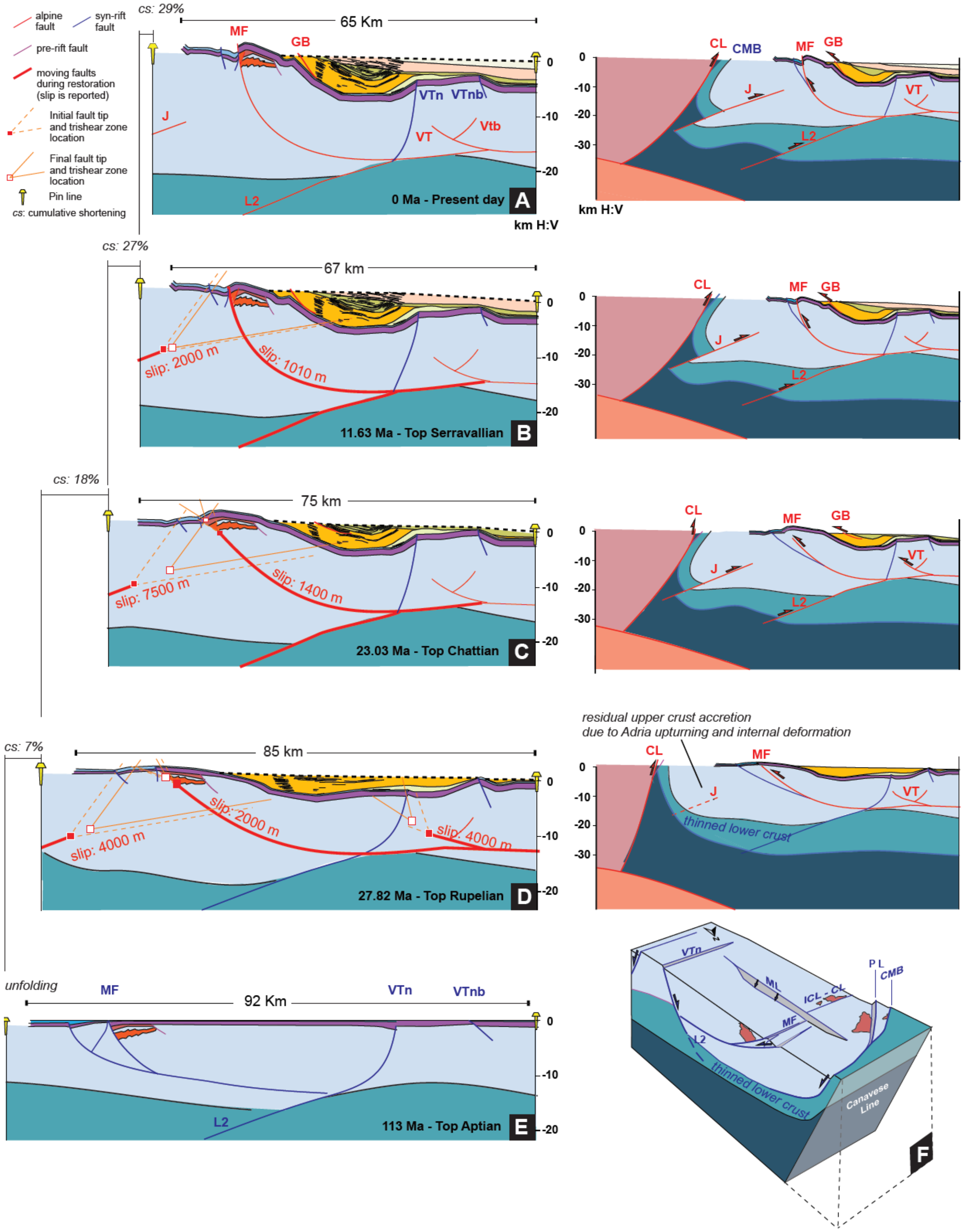

Figure 3: Figure 3: progressive restoration of a simplified version of Varese section (left) and inferred paleo-tectonic transects (right): a) present-day, b) top Serravallian, c) top Chattian, d) top Rupelian, e) top Aptian - end of rifting; f) a schematic 3D block diagram illustrating the crustal architecture at the end of rifting (top of block is the top of basement). Fault codes and units' colors are the same as in Fig. 1.

At the end of rifting (Fig. 3e) the area was characterized by a subsiding sector delimited by the Mesozoic normal faults (see 3D sketch in Fig. 3e). The innermost faults (i.e. the Pogallo, Cossato-Mergozzo and Canavese lines) were responsible for a pronounced thinning of the Adria lower crust. During the first stages of convergence, up to Rupelian (Fig. 3d), a period including the main stages of subduction, deep-seated north-verging thrusting occurred (e.g., Beltrando et al., 2015), coincident with the positive inversion of rift-related normal faults (Marzio Fault) as also observed in the Orobic Alps (Zanchetta et al., 2015). During Chattian times (Fig. 3c) the Villafortuna-Trecate thrust and Marzio Fault continued to take up most of the deformation, but part of the shortening was also accommodated along the J structure, marking the inception of crustal wedge accretion. A dramatic change in the structural style is recorded from Aquitanian onward (Fig. 3a-b), with shortening taken up mostly by the L2 and Marzio Fault structures, whereas the most external structures were inactive. This change in structural style is contemporary to the indentation of Adria beneath the Alps and the associated strike slip motion along the Canavese Line (e.g. Malusà et al., 2016). The internal deformation of the orogenic wedge and crustal accretion is here modeled by the slip on the J structure, whose growth caused the progressive back-tilting of the southern sectors and the closure of the Pedealpine syncline. The shallow accommodation of this folding, in turn, resulted into flexural slip faulting along Gonfolite backthrust that is mostly expressed at surface (i.e., east of Varese) and imaged at depth (Michetti et al., 2012) as a thrust flat. Consistently, earthquakes' *foci* cluster in the sector on top of the J shear zone, and on top of the wedge-related Marzio Fault, where we infer that the most recent crustal deformation focused (i.e., Tortonian – present day). Restoration resulted in 27 km of shortening (i.e., 29% of a restored section of 92 km) for the stack of structures investigated in the Varese area and with much of the slip being spent in uplifting the inner part of the chain through internal deformation, and not by stacking of thin-skinned nappes as previously suggested.

CONCLUSIONS

We discussed the crustal structure of a key area of the Southalpine orogenic wedge, providing a ramp-dominated balanced solution for the accretionary wedge that opposes to previously proposed detachment-dominated interpretations (e.g., Schumacher et al., 1997; Rosenberg and Kissling, 2013; Pfiffner, 2016). The proposed solution depicts the presence of a retro-wedge involving the tip of the north-verging Adria mantle wedge, along with the reactivation of crustal rift-inherited faults and shear zones cutting through previously thinned crustal sectors. The inversion of the deeply rooted normal faults as crustal thrust ramps could related to the inherited thinning of the ductile parts of the continental crust, and the mechanical coupling between the brittle upper crustal and upper lithospheric mantle sections involved in the orogenic wedge (Tavani et al. 2021).

Consistently with Festa et al. (2020), our restoration implies that the Canavese Line acted as a backstop of the subduction-accretion complex, with most of the continental collisional deformation efficiently accommodated inside the wedge through the thickening of the upper crust.

Wedging is documented also in the Orobic Alps, for a pre-Adamello syn-collisional tectonic phase (55-45 Ma: Zanchetta et al., 2015) and came to an apparent pause during Late Eocene - Early Oligocene (42-30 Ma), when Ji et al. (2019) framed a possible phase of slab retreat in the Southern Alps resulting in a higher dip of the slab to the east (ca. 80^{o}) than in the Varese area, where it is close to 60^{o} (Zhao et al., 2016). Here, we conversely documented wedging from Chattian onward, later than on the Orobic Alps and after ceasing of slab retreat. Such a sequence of events, on a broader perspective, suggest that during the collisional and post-collisional history of orogenesis, lithosphere dynamics drove diachronically the onset of tectonic phases (i.e., wedging and slab retreat), from east to west, across the Southern Alps. Even if based on a structural and kinematic approach alone, our results are consistent with a recent numerical thermo-mechanical modeling (Dal Zilio et al. 2020) demonstrating that the rearrangement of forces after a possible breakoff, bending and rollback of the European slab would result in a compressive stress transferred to the shallow crust.

Finally, our work suggests that, in relation to the Orobic stack, i) either the latter represents an upper thrust system, completely eroded in this sector, or ii) a major discontinuity for the change of the basal depth of the contractional wedge could be addressed to the abruptly increase in thickness of Jurassic syn-rift deposits, east of the Lugano-Valgrande fault.

REFERENCES

Beltrando, M., Stockli, D. F., Decarlis, A., and Manatschal, G., 2015, A crustal-scale view at rift localization along the fossil Adriatic margin of the Alpine Tethys preserved in NW Italy: Tectonics, v. 34, no. 9, p. 1927-1951.

Berra, F., Galli, M. T., Reghellin, F., Torricelli, S., and Fantoni, R., 2009, Stratigraphic evolution of the Triassic–Jurassic succession in the Western Southern Alps (Italy): the record of the two-stage rifting on the distal passive margin of Adria: Basin Research, v. 21, no, 3, p. 335-353.

Bertotti, G., Picotti, V., Bernoulli, D., and Castellarin, A., 1993, From rifting to drifting: tectonic evolution of the South-Alpine upper crust from the Triassic to the Early Cretaceous: Sedimentary Geology, v. 86, no. 1-2, p 53-76.

Butler, R. W. and Mazzoli, S., 2006, Styles of continental contraction: A review and introduction: Special papers-Geological Society of America, v. 414, p. 1-11.

Dal Zilio, L., Kissling, E., Gerya, T., and van Dinther, Y., 2020, Slab Rollback Orogeny model: A test-of-concept: Geophysical Research Letters, v. 47, no. 18, e2020GL089917.

Diehl, T., Husen, S., Kissling, E., and Deichmann, N., 2009, High-resolution 3-D P -wave model of the Alpine crust: Geophysical Journal International, v. 179, p. 1133–1147, doi:10.1111/j.1365-246X.2009.04331.x.

Diehl, T., Kissling, E. and Schmid, S, 2017, High-resolution 3D seismic structure of the Ivrea-Verbano Zone, ICDP Baveno Workshop, May 1-5 2017, DOI: 10.13140/RG.2.2.30166.86088

Fantoni, R., Bello, M., Ronchi, P., and Scotti, P., 2002, Po Valley oil play: from the Villafortuna - Trecate field to South-Alpine and Northern Apennine exploration: EAGE Conference Florence, Extended Abstracts Book, p. 1-4.

Fantoni, R. and Scotti, P., 2009, Time of hydrocarbon generation vs trap forming age in Mesozoic oil play in Po Plain: Rendiconti Società. Geologica Italiana,v. 5, p. 89-92.

Festa, A., Balestro, G., Borghi, A., De Caroli, S., and Succo, A., 2020, The role of structural inheritance in continental break-up and exhumation of Alpine Tethyan mantle (Canavese Zone, Western Alps): Geoscience Frontiers, v. 11, p. 167–188, doi:10.1016/j.gsf.2018.11.007.

ISIDe Database (Italian Seismological Instrumental and Parametric Data-Base) v. 1.0: http://terremoti.ingv.it/search (accessed December 2020).

Handy, M.R., Franz, L., Heller, F., Janott, B., and Zurbriggen, R., 1999, Multistage accretion and exhumation of the continental crust (Ivrea crustal section, Italy and Switzerland): Tectonics, v. 18, p. 1154–1177, doi:10.1029/1999TC900034.

Ji, W., Malusà, M.G., Tiepolo, M., Langone, A., Zhao, L., Wu, F., 2019, Synchronous Periadriatic magmatism in the Western and Central Alps in the absence of slab breakoff: Terra Nova, v. 31, no. 2, p. 120–128. https://doi.org/10.1111/ter.12377

Karakas, O., Wotzlaw, J. F., Guillong, M., Ulmer, P., Brack, P., Economos, R., Bergantz, G.W., Sinigoi S., and Bachmann O., 2019. The pace of crustal-scale magma accretion and differentiation beneath silicic caldera volcanoes: Geology, v. 47, no. 8, p. 719-723.

Lescoutre, R. and Manatschal, G., 2020, Role of rift-inheritance and segmentation for orogenic evolution: example from the Pyrenean-Cantabrian system: Bulletin de la Société Géologique de France, v. 191, no. 1.

Malusà, M. G., Anfinson, O. A., Dafov, L. N., and Stockli, D. F., 2016, Tracking Adria indentation beneath the Alps by detrital zircon U-Pb geochronology: Implications for the Oligocene–Miocene dynamics of the Adriatic microplate: Geology, v. 44, no. 2, p. 155-158.

Mazzucchelli, M., Quick, J. E., Sinigoi, S., Zanetti, A., and Giovanardi, T., 2014, Igneous evolutions across the Ivrea crustal section: The Permian Sesia Magmatic System and the Triassic Finero intrusion and mantle: Goldschmidt conference–Florence, 2013: Geological Field Trips, v. 6, no, 2.2, p. 98, doi: 10.3301/GFT.2014.05.

Michetti, A., Giardina, F., Livio, F., Mueller, K., Serva, L., Sileo, G., Vittori, E., Devoti, R., Riguzzi, F., Carcano, C., Rogledi, S., Bonadeo, L., Brunamonte, F., and Fioraso, G., 2012, Active compressional tectonics, Quaternary capable faults, and the seismic landscape of the Po Plain (N Italy): Annals of Geophysics, v. 55, no. 5, p. 969.1001, doi: 10.4401/ag-5462.

Mitra, S., and Miller, J. F., 2013, Strain variation with progressive deformation in basement-involved trishear structures. Journal of Structural Geology, v. 53, p. 70-79.

Pfiffner, O. A., 2016, Basement-involved thin-skinned and thick-skinned tectonics in the Alps: Geological Magazine, v. 153, no. 5-6, p. 1085-1109.

Pfiffner, O. A., Lehner, P., Heitzmann, P., Mueller, S., and Steck, A., 1997, Deep structure of the Swiss Alps: results of NRP 20, Basel, Birkhäuser, Switzerland, 380 p.

Pohl, F. et al. (2018): Kinematics and Age of Syn-Intrusive Detachment Faulting in the Southern Alps: Evidence for Early Permian Crustal Extension and Implications for the Pangea A Versus B Controversy. Tectonics, 37 (10). pp. 3668-3689. DOI 10.1029/2018TC004974.

Roda, M., Regorda, A., Spalla, M. I., and Marotta, A. M., 2019, What drives Alpine Tethys opening? Clues from the review of geological data and model predictions: Geological Journal, v. 54, no. 4, p. 2646-2664.

Rosenberg, C. L., and Kissling, E., 2013, Three-dimensional insight into Central-Alpine collision: Lower-plate or upper-plate indentation?: Geology, v. 41, no. 12, p. 1219-1222.

Schaltegger, U., and Brack, P., 2007, Crustal-scale magmatic systems during intracontinental strike-slip tectonics: U, Pb and Hf isotopic constraints from Permian magmatic rocks of the Southern Alps: International Journal of Earth Sciences, v. 96, p. 1131–1151, doi: 10 .1007 /s00531 -006 -0165 -8 .

Schmid, S.M., Kissling, E., Diehl, T., van Hinsbergen, D.J.J., and Molli, G., 2017, Ivrea mantle wedge, arc of the Western Alps, and kinematic evolution of the Alps–Apennines orogenic system: Swiss Journal of Geosciences, v. 110, p. 581–612, doi:10.1007/s00015-016-0237-0.

Schmid, S.M., Pfiffner, O.A., Froitzheim, N., Schönborn, G., and Kissling, E., 1996: Geophysical-geological transect and tectonic evolution of the Swiss-Italian Alps: Tectonics, v. 15, p. 1036–1064, doi:10.1029/96TC00433.

Schmid, S. M., Zingg, A., and Handy, M., 1987, The kinematics of movements along the Insubric Line and the emplacement of the Ivrea Zone: Tectonophysics, v. 135, no. 1-3, p. 47-66.

Schumacher, M.E., Schönborn, G., Bernoulli, D., and Laubscher, H.P., 1997, Rifting and collision in the Southern Alps, in Pfiffner, Q.A., et al., eds., Deep Structure of the Swiss Alps—Results from the National Research Program 20 (NRP 20): Basel, Birkhäuser, p. 186–204.

Spada, M., Bianchi, I., Kissling, E., Piana, Agostinetti N., and Wiemer, S., 2013, Combining controlled-source seismology and receiver function information to derive 3-D Moho topography for Italy: Geophysical Journal International, v. 194, no.2, p. 1050–1068, doi: 10.1093/gji/ggt148.

Tavani, S., Granado, P., Corradetti, A., Camanni, G., Vignarol, G., Manatschal, G., Mazzoli, S., Muñoz, J.A. and Parente, M. 2021, Rift inheritance controls the switch from thin- to thick-skinned thrusting and basal décollement re-localization at the subduction-to-collision transition: Geological Society of America Bulletin, https://doi.org/10.1130/B35800.1 (in press)

Tremolada, F., Guasti, E., Scardia, G., Carcano, C., Rogledi, S., and Sciunnach, D., 2010, Reassessing the biostratigraphy and the paleobathymetry of the Gonfolite Lombarda Group in the Como area (northern Italy): Rivista Italiana di Paleontologia e Stratigrafia, v. 116, no. 1, p. 35-49, doi: 10.13130/2039-4942/5939.

Zanchetta, S., Malusà, M.G., Zanchi, A.M., 2015, Pre-collisional development and Cenozoic evolution of the Southalpine retrobelt (European Alps): Lithosphere, v. 7, no. 6, p 662-681.https://doi.org/10.1130/L466.1

Zehnder, A. T., and Allmendinger, R. W., 2000, Velocity field for the trishear model: Journal of Structural Geology, v. 22, no. 8, p. 1009-1014, doi: 10.1016/S0191-8141(00)00037-7.

Zhao, L., Paul, A., Malusà, M.G., Xu, X., Zheng, T., Solarino, S., Guillot, S., Schwartz, S., Dumont, T., Salimbeni, S., Aubert, C., Pondrelli, S., Wang, Q., Zhu, R., 2016. Continuity of the Alpine slab unraveled by high-resolution P wave tomography: Continuity of the Alpine

Slab. Journal of Geophysical Research: Solid Earth, v. 121, no. 12, p. 8720–8737. https://doi.org/10.1002/2016JB013310

APPENDIX 1: METHODS

We restored the Varese section using the 2D Move-on-fault and 2D Unfolding modules of the MOVE suite by Petex Inc.

Fault propagation folds have been restored by means of a trishear numerical code (i.e., Erslev, 1991; Hardy and Ford, 1997; Zehnder & Allmendinger, 2000).

The trishear model describes the deformation induced by a growing fault as a triangular zone of shear emanating from the tip of a propagating fault (Figure 1). The algorithm deforms beds in a single (homogenous trishear), or series of nested, triangular zone(s) of shear (heterogenous trishear), where the magnitude of slip is varied from a user defined value at the top of the zone to zero at the base of the zone and the direction of slip is varied from parallel to the fault dip at the top of the zone to parallel to the base of the zone at the lower boundary of the zone (Hardy and Ford, 1997). We here adopted only a homogenous trishear model: the only parameter defining the triangular velocity field is the trishear angle offset (Figure 1): a value indicating the fraction of the triangular area comprised between the fault projection and the upper trishear boundary. Other variables that can be controlled are the apical angle (or angle between the boundaries of the trishear zone; a in Figure 1), fault dip (b in Figure 1), slip and the propagation to slip ratio (p/s ratio; Figure 1). Area is preserved within the zone during deformation.

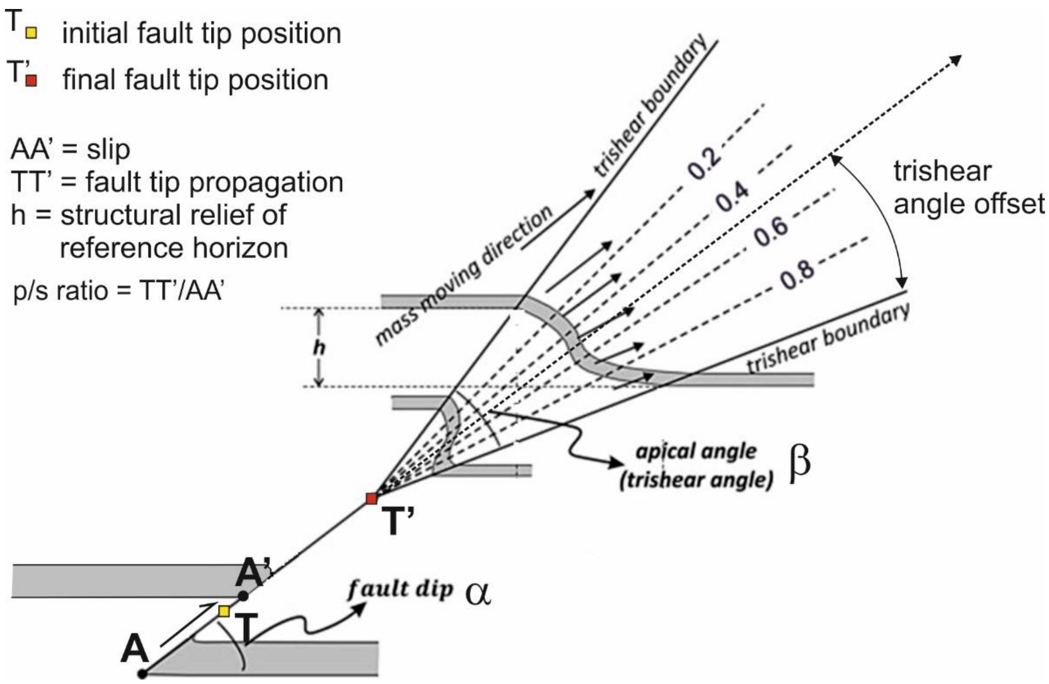

Figure 4: the trishear kinematic model (modified after Pei et al., 2014) with the possible parameters to be set.

Given a fault of a certain geometry, the slip is determined by the structural relief of a reference horizon across the fault (h in Figure 1) and outside the trishear zone whereas the remaining parameters (i.e., apical angle b, p/s ratio and trishear angle) need to be fine-tuned in order to restore the reference horizon to a viable pre-deformative geometry. We moved the hanging wall sector of each thrust moved along the fault according to a fault-parallel flow model (Egan et al., 1997; Kane et al., 1997). This algorithm assumes particle flow parallel to the fault surface and parallel to the plane of cross-section (plane strain assumption). Compared to other geometric construction models like those predicted by fault bend fold theory, the fault parallel flow is not restricted to simple ramp-flat-ramps with a dip less than 30° thus, may be better applied to faults with a complex geometry or curved hinge sectors.

For unfolding, we adopted a flexural slip algorithm, that uses a pin and a slip-system parallel to the template bed to control the unfolding of the remaining horizons.

In the following we'll give the complete parametrization of the trishear restoration modeling, for each of the faults that moved during each of the restoration steps.

First step (present day – top Serravallian).

J was restored according to a trishear kinematic model with the parameters indicated in Table 1. The fault J was moved with a slip of 2000 m in order to place the hanging wall sector at the same elevation of the top Serravallian reference horizon (i.e., no sedimentation room in the chain sector). This assumption comes from the consideration that foredeep deposits were not present in these sectors of the chain. We thus adopted a fill-to-the-top approach (i.e., the structural relief of the structure compensated the thickness of the syn-growth sequence deposited in the basin) thus reaching an estimation of the maximum value of slip for the considered time window.

MF was restored according to a fault parallel flow model by restoring the offset of the Aptian unconformity (i.e., a reference horizon for the end-of-rifting stage) and by obtaining a viable geometry for the top Serravallian reference horizon. Faults geometries, fault tip initial and final positions and trishear zone migration are illustrated in Figure 2.

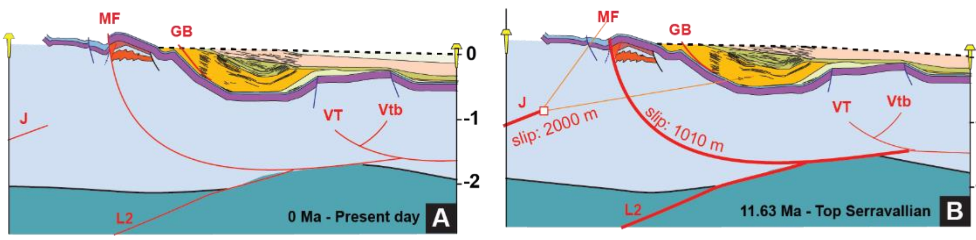

Figure 2 – First step of restoration: from present day (A) to the top of Serravallian (B); faults that moved during this step are drawn with thick red lines and the location of the trishear zone is also indicated.

Fault code	Apical angle b (degrees)	Trishear angle offset	p/s ratio	Slip (m)
J	45	0.73	1.5	2000
MF (fault parallel flow)	-	-	-	1010

Table 1: parameters adopted for step 1 of the restoration.

Second step (top Serravallian – top Chattian).

Both J and MF were restored by means of a trishear kinematic model with the parameters indicated in Table 2. Slip and parameters were estimated in order restore a top Chattian reference horizon and adopting a fill-to-the-top assumption. Faults geometries, fault tip initial and final positions and trishear zone migration are illustrated in Figure 3.

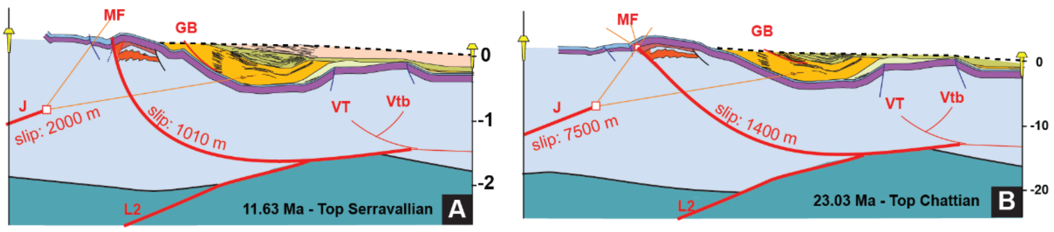

Figure 3 –Second step of restoration: from top Serravallian (A) to the top of Chattian (B); faults that moved during this step are drawn with thick red lines and the location of the trishear zone is also indicated.

Fault code	Apical angle b (degrees)		Trishear angle offset	p/s ratio	Slip (m)
J	50		0.80	1	7500
MF	40		0.60	1.5	1400

Table 2: parameters adopted for step 2 of the restoration.

Third step (top Chattian – top Rupelian).

Both J and MF were restored by means of a trishear kinematic model with the parameters indicated in Table 3. Slip and parameters were estimated in order restore a top Chattian reference horizon and adopting a fill-to-the-top assumption. Faults geometries, fault tip initial and final positions and trishear zone migration are illustrated in Figure 4.

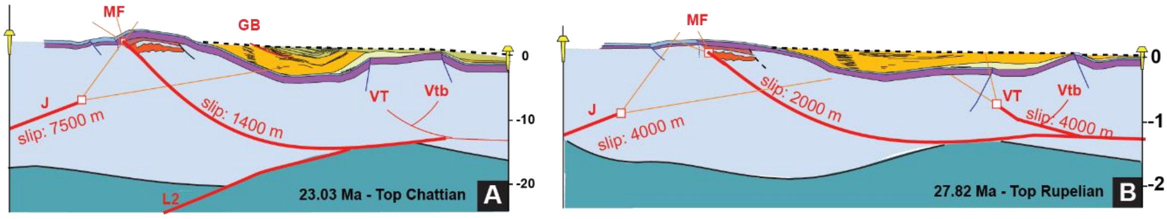

Figure 4 –Third step of restoration: from top Chattian (A) to the top of Rupelian (B); faults that moved during this step are drawn with thick red lines and the location of the trishear zone is also indicated.

Fault code	Apical angle b (degrees)	Trishear angle offset	p/s ratio	Slip (m)
J	46	0.71	1	4000
MF	50	0.54	1.5	2000
VT	37	0.60	1	4000

Table 3: parameters adopted for step 3 of the restoration.

Fourth step (top Rupelian – top Aptian; end of rifting).

All the remaining deformation was restored by means of a 2D unfolding approach. Faults geometries, fault tip initial and final positions and trishear zone migration are illustrated in Figure 5.

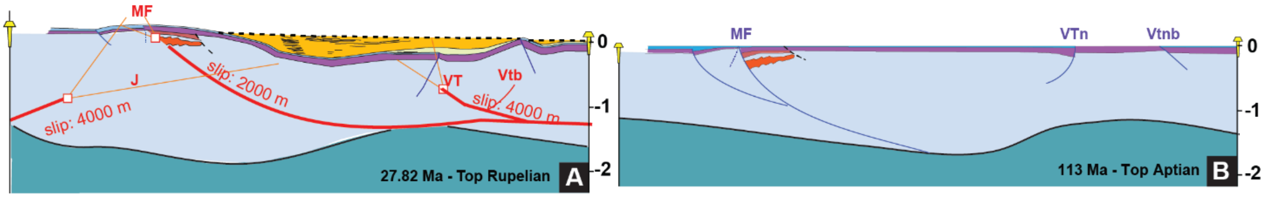

Figure 5 –Fourth step of restoration: from top Rupelian (A) to the top of Aptian (B); faults that moved during this step are drawn with thick red lines and the location of the trishear zone is also indicated.

Appendix References:

Egan, S. S., Buddin, T. S., Kane, S. J., and Williams, G. D., 1997, Three-dimensional modelling and visualization in structural geology: New techniques for the restoration and balancing of volumes, In: Proceedings of the 1996 Geoscience Information Group Conference on Geological Visualisation: Electronic Geology, V. 1, Paper 7, p.67-82.

Erslev, E. A., 1991. Trishear fault-propagation folding: Geology, 19, p.617-620.

Hardy, S. and Ford, M., 1997, Numerical modelling of trishear fault-propagation folding and associated growth strata: Tectonics, 16, p.841-854.

Kane, S. J., Williams, G. D., Buddin, T. S., Egan, S. S., and D. Hodgetts, 1997, Flexural-slip based restoration in 3D, a new approach: 1997 AAPG Annual Convention Official Program, A58.

Pei, Y., Paton, D. A., & Knipe, R. J. (2014). Defining a 3-dimensional trishear parameter space to understand the temporal evolution of fault propagation folds. Journal of structural Geology, 66, 284-297.

Zehnder, T. A. and Allmendinger, R. W., 2000, Velocity field for the trishear model: Journal of Structural Geology, 22, p.1009-1014.